PHYSICAL REVIEW B **92**, 060406(R) (2015)

# Single-photon level study of microwave properties of lithium niobate at millikelvin temperatures

Maxim Goryachev, Nikita Kostylev, and Michael E. Tobar*

*ARC Centre of Excellence for Engineered Quantum Systems, School of Physics, University of Western Australia, 35 Stirling Highway, Crawley WA 6009, Australia*

(Received 28 April 2015; revised manuscript received 2 July 2015; published 10 August 2015)

The properties of doped and natural impurities in lithium niobate single crystals are studied using the whispering gallery mode method at low temperatures as a function of magnetic field. The study reveals considerable coupling of microwave photon modes to the $Fe^{3+}$ spin ensemble in iron-doped and nondoped crystals. The $S = 5/2$ structure of the $Fe^{3+}$ impurities demonstrates zero field splittings of 11.21 and 20.96 GHz, a significant asymmetry of the Zeeman lines, and additional lines with anomalous $g$ factors of 1.37 and 3.95. Also, interactions between different transitions of the $Fe^{3+}$ ion are observed. An additional ion impurity ensemble with a splitting of about 1.7 GHz is shown to couple to the dominating $Fe^{3+}$ spins, and the effect on the $Q$ factors of the microwave photon modes due to the $Fe^{3+}$ ion ensemble is also demonstrated. Measurements down to less than one photon level are made, with a loss tangent of order $10^{-5}$ determined.

DOI: 10.1103/PhysRevB.92.060406 PACS number(s): 78.70.Gq, 42.50.Pq, 42.70.Mp, 07.57.Pt

Quantum system technology is a rapidly growing field that promises a new generation of sensing, computing, and data transfer. For the last couple of decades, a variety of approaches to quantum technology has been developed, including superconducting qubits, trapped ions, ions in solids, optomechanics, etc. All of these directions have their advantages and disadvantages. As a result, the concept of a hybrid quantum system (HQS) has been proposed and developed [1]. The concept of an HQS is not only supposed to overcome disadvantages of standalone quantum technologies, but also to couple them into a single network. An example of this is microwave-to-optical conversion with quantum efficiency [2–4] that may be used to unify spatially separated superconducting quantum processing units into a whole network via optical links. More generally, for perspective quantum devices, the problem of the combination of optical and microwave subsystems is important at the current stage of technology development.

The discussed optical-microwave coupling may be constructed using mechanical devices coupled simultaneously to optical and microwave cavities [5,6], with a spin ensemble exhibiting both microwave and optical transitions [1,7,8], with media consisting of nontrivial properties in the two parts of the spectrum or with some dielectric phenomena, e.g., the electro-optic effect [9]. The success or failure of any of these approaches depends considerably on the material properties determining whether or not the system photons have enough time to interact before being lost or dephased. Thus, it is vital to understand the microwave and optical properties of perspective materials at low temperatures and low excitation levels. The latter condition is shown to be important for ultrahigh quality dielectric materials where losses are determined by microwave photons interacting with impurity paramagnetic spin ensembles [10,11]. These unavoidable ion ensembles with concentrations as low as parts per $10^9$ (ppb) introduce the power dependence of the loss rate such that low excitation level experiments demonstrate lower quality factors. On the other hand, intrinsic spin ensembles themselves may be used as a part of an HQS. To investigate this possibility, the spin-photon interaction properties have to be characterized under the same conditions.

The double frequency band nature of the problem requires the use of materials that demonstrate equally good properties in optical and microwave domains at low temperatures, although usually there is a lack of information about the microwave properties of the optical materials and vice versa. This happens because the typical working solutions in one field demonstrate considerable disadvantages in another and thus do not suit the combined system. To cover this gap between the two kingdoms, we investigate a known material with recognized nontrivial optical properties, namely, lithium niobate ($LiNbO_3$) [12], in the microwave frequency range and at millikelvin temperatures. Lithium niobate is a popular crystal with a large dielectric constant (up to 85, depending on the direction) and an electro-optic coefficient (up to 33 pm/V) used for various optical applications, including optical modulation, optical waveguides, and high-$Q$ microdisk resonators [13,14] exhibiting nonlinear phenomena [15] including attempts to create microwave-to-optics conversions with a quantum level efficiency [2]. On the other hand, despite some work [16–20], the mechanical, microwave, and optical properties of this material at low temperatures and low excitation levels still need to be studied in detail.

In this Rapid Communication, the microwave properties of $LiNbO_3$ single crystals are studied using the whispering gallery mode (WGM) approach. This approach has been demonstrated to provide very accurate data for the dielectric properties of low loss materials [21] and ultrasensitive spectroscopy of naturally occurring [22–25] and doped [25–27] ion impurities. Depending on material losses, this technique can detect ion ensembles with concentrations down to a few ppb at multiple frequencies in the $X$ and $K_u$ bands (5–25 GHz). Additionally, WGMs are a nice tool to observe various nonlinear phenomena related to dielectrics and spin ensembles, such as four-wave mixing and masing [28,29]. The advantages of the WGM technique are a high filling factor (due to the fact that the microwave cavity is simultaneously a host for the spin ensemble) and high quality factors. The obtained results may be used to decide on whether a particular spin ensemble may be used for quantum electrodynamics (QED) experiments and

*michael.tobar@uwa.edu.au

 

what spectrum regions have to be avoided to minimize photon losses due to two-level system absorption.

The experiments are performed with two cylindrical single crystals: undoped $LiNbO_3$ and iron-doped $LiNbO_3$ ($Fe^{2+}$,$Fe^{3+}$ ions with 0.005 wt %), with the $c$ axis of the crystal aligned with the $z$ axis of the cylinder (the crystal exhibits biaxial anisotropy). Both crystals are 15 mm long and 15 mm in diameter with a 1 mm hole in the center for the metallic support structure. Crystals are enclosed in a closed oxygen-free copper structure with two straight probe coupling antennas. The whole system is placed in the center of a 7 T superconducting magnet and thermally grounded to a 20 mK stage of a dilution cryogenerator. The spectroscopy is performed via a network analysis with the room temperature signal attenuated by a series of cryogenic attenuators (−40 dB at different cryocooler stages). The output signal passes through low noise amplifiers both at 4 K and at room temperature. The cavity and the cryogenic amplifier are separated by a millikelvin circulator to prevent the back action noise from the 4 K stage of the amplifier. The setup is similar to previous QED experiments with WGM and other microwave cavities [24,30].

Resonance frequencies of the WGMs of cylindrical crystals are set by the cavity dimensions and the dielectric and magnetic properties of the material. In the case of paramagnetic spin ensemble impurities within the crystal, the external magnetic field changes the energy level splitting due to the Zeeman effect. When the splitting frequency coincides with the resonance frequency of one of the system WGMs, the latter exhibits some frequency and linewidth deviation. So, in order to reveal the ion spin level structure, we construct a map of interactions where each point represents an interaction frequency and the corresponding magnetic fields. The interaction maps for the doped and undoped lithium niobate are shown in Figs. 1 and 2, correspondingly.

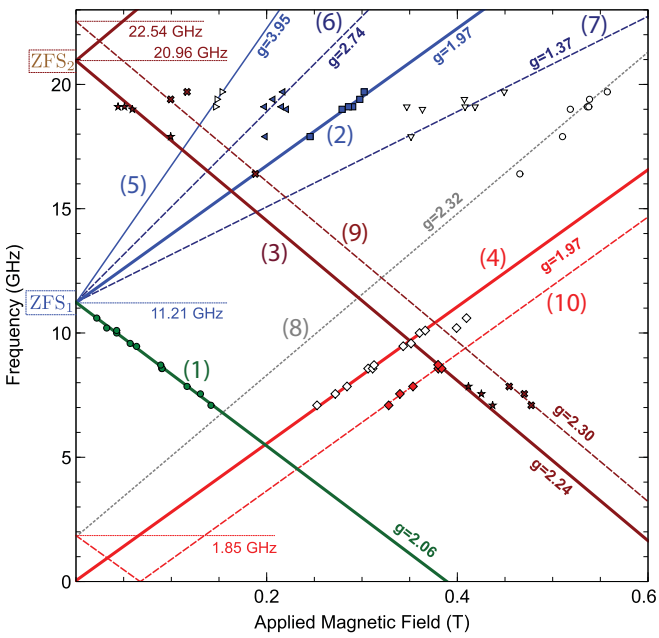


FIG. 1. (Color online) Spectroscopy results for the Fe:$LiNbO_3$ crystal. Point objects mark experimentally observed points of interaction. The lines demonstrate their interpretation in terms of the Zeeman tuning of transitions in ion ensembles.

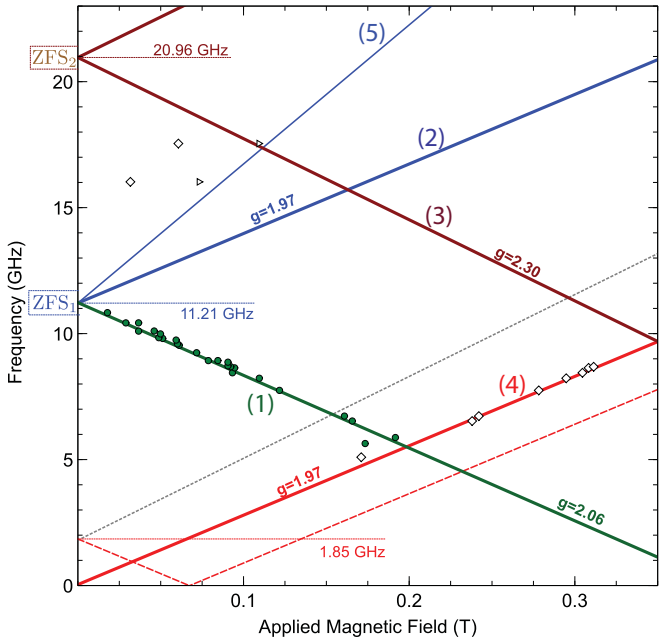


FIG. 2. (Color online) Spectroscopy results for the undoped $LiNbO_3$ crystal. Lines are fits for the Fe:$LiNbO_3$ crystal,

The experimental data shown in Fig. 1 reveal a zero field splitting (ZFS) structure ($ZFS_1$ and $ZFS_2$) with Zeeman lines (1)–(5) that may be interpreted as the transition structure between energy levels of $Fe^{3+}$ ions [31,32]. Here, line (5) is a two-photon transition ($\Delta S_m = 2$) with a $g$ factor twice of that of line (2). By fitting two ZFSs (11.21 and 20.96 GHz), one finds the spin parameter $D = 5.33$ GHz that approximately corresponds to that predicted before [32].

Despite the good agreement of the ZFS parameters with previous results, the spin ensemble also demonstrates a few distinct features that have not been observed at higher temperatures. First, the $g$ factors for the Zeeman lines with positive and negative directions have different sign corrections to the electron $g$ factor in vacuum, making the splitting slightly asymmetric. This property has been also observed for natural impurities in quartz [23]. Second, besides two Zeeman lines (2) and (5) representing the expected one- and two-photon transitions, the map of interactions demonstrates the existence of two more lines with the same ZFS [lines (6) and (7)]. Since the ratio of the $g$ factors of these lines is two, they represent one- and two-photon transitions of the same ion energy splitting. On the other hand, their values (1.37 and 3.95) are significantly different from the multiples of the vacuum electron spin $g$ factor that is unusual for iron group ions in crystals. The origin of these Zeeman lines cannot be explained by the traditional spin Hamiltonian of $Fe^{3+}$ ions in solids. Third, Zeeman lines (8)–(10) with ZFSs of 1.85 and 22.54 GHz do not correspond to any transition of the $Fe^{3+}$ $S = 5/2$ structure and are most likely another spin ensemble. It can be noted that line (10) is related to line (4) by a similar amount (1.85 GHz) of zero field frequency shift as line (9) to line (3) (1.55 GHz) also corresponding to the ZFS of line (8). This might be explained by the coupling of the $Fe^{3+}$ to some other ion species with a corresponding ZFS. A similar phenomenon

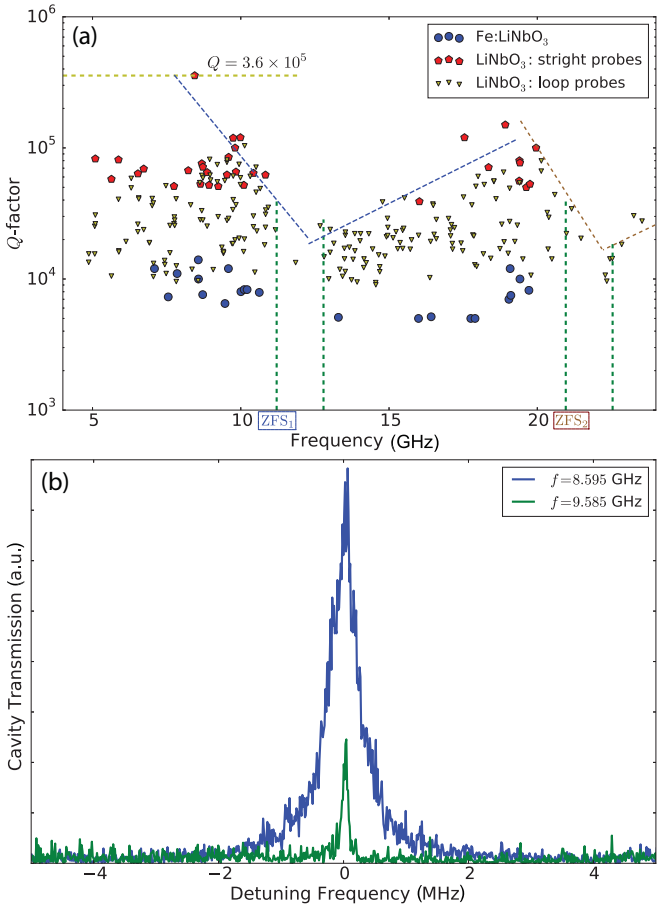


FIG. 3. (Color online) (a) $Q$ factors of WGMs used for impurity spectroscopy. (b) Mode shapes of two WGMs measured at less than one stored photon.

for $Fe^{3+}$ and $V^{2+}$ has been proposed to explain the extra hyperfine structure in sapphire [22]. The presence of other iron group ions such as $Cr^{3+}$ [33], $Mn^{2+}$ [34], and $Cu^{2+}$ [35] in $LiNbO_3$ at room temperature have been studied at room temperature. On the other hand, iron ions themselves can come with different site centers, giving rise to much smaller crystal field parameters: $b_2^0 = 1.5$ and 2.1 GHz [31] and $b_2^0 = 0.46$ and 0.6 GHz [36].

Spectroscopy results for the undoped crystal clearly demonstrated only two transition lines (Fig. 1). These transitions correspond to lines (1) and (4) of the doped crystal. This fact demonstrates some natural abundance of iron in $LiNbO_3$.

The relation between paramagnetic impurities and microwave losses is well known [10,11]. This relation may be observed via the quality factors of microwave WGMs. Figure 3(a) displays $Q$ factors for WGMs for both doped and undoped crystals over the available frequency band. The plot shows that losses in the doped sample are about an order of magnitude higher than in the undoped crystal. The other important detail is the relation between the first ZFS and the observed spectrum: The mode density drops significantly immediately above ZFS$_1$, making a gap in the mode spectrum. Measurements of the cavity transmission as a function of the driving power demonstrated no clear dependence on the number of stored cavity photons. Figure 3(b) demonstrates the

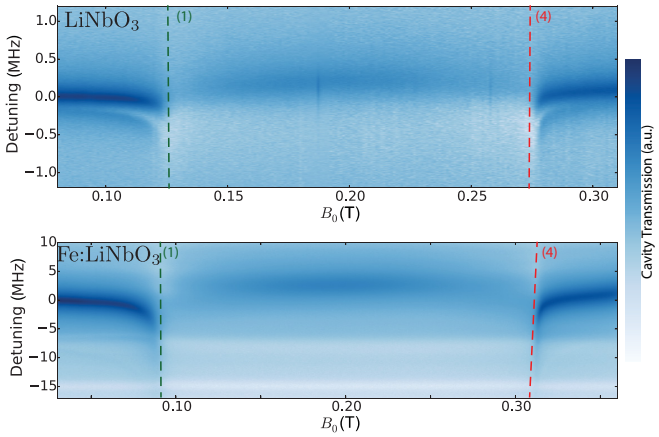


FIG. 4. (Color online) Frequency response of doped and undoped crystals as a function of external magnetic field $B_0$ in close proximity between spin transitions (1) and (4).

cavity transmission near two WGMs measured with less than one stored photon on average [10].

Another important feature of $Fe^{3+}$ ions in lithium niobite is the strong influence of different transitions on each other. This property can be important for QED type experiments. In previous experiments with low doped crystals [22–25], each interaction is well approximated by an avoided level crossing (ALC) between an ensemble of a two-level system (TLS) and a harmonic oscillator (HO). For the iron ensemble in lithium niobite, the situation is different, as depicted in Fig. 4, where interaction lines (1) and (4) display intercoupling resulting in ALC suppression. This situation can be modeled by a cavity mode $a^\dagger a$ interacting with two TLS ensembles with non-negligible intercoupling:

$$H = \omega_c a^\dagger a + \sum_i \left[\omega_{a1}\sigma_{1i}^z + \omega_{a2}\sigma_{2i}^z + \lambda(\sigma_{1i}^+\sigma_{2i}^- + \sigma_{2i}^+\sigma_{1i}^-) + g_i(\sigma_{1i}^+ a + a^\dagger\sigma_{1i}^- + \sigma_{2i}^+ a + a^\dagger\sigma_{2i}^-)\right], \quad (1)$$

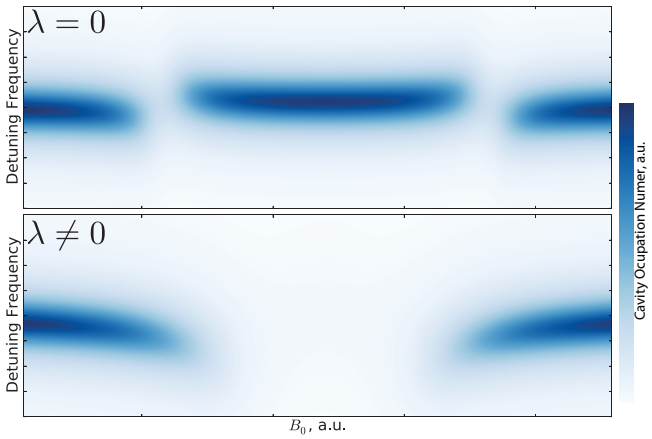


FIG. 5. (Color online) Modeling of the cavity mode interaction with two ion transitions corresponding to $\lambda = 0$ of different ions, and $\lambda \neq 0$ of the same ion.

where $\sigma_{ni}^{+}$, $\sigma_{ni}^{+}$, and $\sigma_{ni}^{+}$ are the usual spin operators for the $n$th transition of the $i$th ion, and $\lambda$ is the intertransition coupling. The frequency response of this system including its couplings to the environment is simulated using QUTIP [37,38]. The result shown in Fig. 5 displays the cavity occupation number as a function of the pump frequency and external magnetic field in two cases: independent ion transitions ($\lambda = 0$) and the same ion transitions ($\lambda \neq 0$). The simulation clearly demonstrates that the interaction with the transitions of the same ion may lead to the disappearance of ALCs even if they are separated by more than the ion-cavity coupling strength.

In summary, we have investigated single-photon level properties of iron-doped and undoped lithium niobate at millikelvin temperatures with WGMs. The microwave spectroscopy confirms the existence of $Fe^{3+}$ with large ZFSs and some traces even in undoped crystals. None of the observed interactions in the low and high spin concentration regimes demonstrate the spin-photon strong coupling regime suitable for QED experiments [39] due to high spin losses and a strong influence of the different ion transitions on each other. This problem cannot be solved by additional doping as it leads to higher spin ensemble losses. On the other hand, the influence of the impurity spin ensemble on photon modes is revealed via $Q$ factors and mode density that has to be taken into account when designing electro-optical single-photon devices. The observed quality factors are of the order of $10^5$, which is still below the state-of-the art superconducting systems [40,41]. An additional structure with a characteristic splitting of 1.85–1.55 GHz suggests the existence of another coupled spin ensemble.

[1] A. M. Stephens, J. Huang, K. Nemoto, and W. J. Munro, Phys. Rev. A **87**, 052333 (2013).
[2] D. V. Strekalov, H. G. L. Schwefel, A. A. Savchenkov, A. B. Matsko, L. J. Wang, and N. Yu, Phys. Rev. A **80**, 033810 (2009).
[3] S. Barzanjeh, M. Abdi, G. J. Milburn, P. Tombesi, and D. Vitali, Phys. Rev. Lett. **109**, 130503 (2012).
[4] L. Tian, P. Rabl, R. Blatt, and P. Zoller, Phys. Rev. Lett. **92**, 247902 (2004).
[5] K. Stannigel, P. Rabl, A. S. Sørensen, P. Zoller, and M. D. Lukin, Phys. Rev. Lett. **105**, 220501 (2010).
[6] R. W. Andrews, R. W. Peterson, T. P. Purdy, K. Cicak, R. W. Simmonds, C. A. Regal, and K. W. Lehnert, Nat. Phys. **10**, 321 (2014).
[7] C. O'Brien, N. Lauk, S. Blum, G. Morigi, and M. Fleischhauer, Phys. Rev. Lett. **113**, 063603 (2014).
[8] L. A. Williamson, Y.-H. Chen, and J. J. Longdell, Phys. Rev. Lett. **113**, 203601 (2014).
[9] M. Tsang, Phys. Rev. A **81**, 063837 (2010).
[10] D. L. Creedon, Y. Reshitnyk, W. Farr, J. M. Martinis, T. L. Duty, and M. E. Tobar, Appl. Phys. Lett. **98**, 222903 (2011).
[11] J. G. Hartnett, M. E. Tobar, and J. Krupka, J. Phys. D **34**, 959 (2001).
[12] *Properties of Lithium Niobate*, edited by K. K. Wong, EMIS Datareviews Series No. 28 (The Institution of Engineering and Technology, London, 2002).
[13] J. Lin, Y. Xu, Z. Fang, M. Wang, J. Song, N. Wang, L. Qiao, W. Fang, and Y. Cheng, Sci. Rep. **5**, 8072 (2015).
[14] J. U. Fürst, D. V. Strekalov, D. Elser, M. Lassen, U. L. Andersen, C. Marquardt, and G. Leuchs, Phys. Rev. Lett. **104**, 153901 (2010).
[15] P. Ferraro, S. Grilli, and P. D. Natale, *Ferroelectric Crystals for Photonic Applications*, Springer Series in Materials Science Vol. 91 (Springer, Berlin, 2009).
[16] J. D. Morse, K. G. McCammon, C. F. McConaghy, D. A. Masquelier, H. E. Garrett, and M. E. Lowry, Proc. SPIE **2150**, 283 (1994).
[17] S. L. Bravina, A. N. Morozovska, N. V. Morozovsky, and Y. A. Skryshevsky, Ferroelectrics **298**, 31 (2004).
[18] C. Herzog, G. Poberaj, and P. Günter, Opt. Commun. **281**, 793 (2008).
[19] A. Dhar, N. Singh, R. K. Singh, and R. Singh, J. Phys. Chem. Solids **74**, 146 (2013).
[20] W. R. Huang, S.-W. Huang, E. Granados, K. Ravi, K.-H. Hong, L. E. Zapata, and F. X. Kärtner, J. Mod. Opt. (2014).
[21] J. Krupka, K. Derzakowski, M. Tobar, J. Hartnett, and R. G. Geyer, Meas. Sci. Technol. **10**, 387 (1999).
[22] W. G. Farr, D. L. Creedon, M. Goryachev, K. Benmessai, and M. E. Tobar, Phys. Rev. B **88**, 224426 (2013).
[23] M. Goryachev, W. G. Farr, and M. E. Tobar, Appl. Phys. Lett. **103**, 262404 (2013).
[24] M. Goryachev, W. G. Farr, D. L. Creedon, and M. E. Tobar, Phys. Rev. B **89**, 224407 (2014).
[25] M. Goryachev, W. G. Farr, N. do Carmo Carvalho, D. L. Creedon, J.-M. Le Floch, S. Probst, P. Bushev, and M. E. Tobar, Appl. Phys. Lett. **106**, 232401 (2015).
[26] W. G. Farr, M. Goryachev, D. L. Creedon, and M. E. Tobar, Phys. Rev. B **90**, 054409 (2014).
[27] W. G. Farr, M. Goryachev, J. M. Le Floch, P. Bushev, and M. E. Tobar, arXiv:1412.0086.
[28] J. Bourhill, K. Benmessai, M. Goryachev, D. L. Creedon, W. Farr, and M. E. Tobar, Phys. Rev. B **88**, 235104 (2013).
[29] D. L. Creedon, K. Benmessaï, W. P. Bowen, and M. E. Tobar, Phys. Rev. Lett. **108**, 093902 (2012).
[30] M. Goryachev, W. G. Farr, D. L. Creedon, Y. Fan, M. Kostylev, and M. E. Tobar, Phys. Rev. Appl. **2**, 054002 (2014).
[31] G. I. Malovichko, V. G. Grachev, O. F. Schirmer, and B. Faust, J. Phys.: Condens. Matter **5**, 3971 (1993).
[32] D. J. Keeble, M. Loyo-Menoyo, Y. Furukawa, and K. Kitamura, Phys. Rev. B **71**, 224111 (2005).
[33] T. H. Yeom, Y. M. Chang, C. Rudowicz, and S. H. Choh, Solid State Commun. **87**, 245 (1993).
[34] S. K. Misra and J. Sun, Magn. Reson. Rev. **16**, 57 (1991).
[35] S. K. Misra and C. Wang, Magn. Reson. Rev. **14**, 157 (1990).
[36] H. A. Buckmaster and D. B. Delay, Magn. Reson. Rev. **3**, 127 (1974).
[37] J. Johansson, P. Nation, and F. Nori, Comput. Phys. Commun. **183**, 1760 (2012).
[38] J. Johansson, P. Nation, and F. Nori, Comput. Phys. Commun. **184**, 1234 (2013).

[39] R. Amsüss, C. Koller, T. Nöbauer, S. Putz, S. Rotter, K. Sandner, S. Schneider, M. Schramböck, G. Steinhauser, H. Ritsch, J. Schmiedmayer, and J. Majer, Phys. Rev. Lett. **107**, 060502 (2011).

[40] A. Megrant, C. Neill, R. Barends, B. Chiaro, Y. Chen, L. Feigl, J. Kelly, E. Lucero, M. Mariantoni, P. J. J. O'Malley, D. Sank, A. Vainsencher, J. Wenner, T. C. White, Y. Yin, J. Zhao, C. J. Palmstrøm, J. M. Martinis, and A. N. Cleland, Appl. Phys. Lett. **100**, 113510 (2012).

[41] H. Paik, D. I. Schuster, L. S. Bishop, G. Kirchmair, G. Catelani, A. P. Sears, B. R. Johnson, M. J. Reagor, L. Frunzio, L. I. Glazman, S. M. Girvin, M. H. Devoret, and R. J. Schoelkopf, Phys. Rev. Lett. **107**, 240501 (2011).